11-2016

Enhanced Flow Boiling Heat Transfer in Radial Microchannel and Offset Strip Fin Geometries

Alyssa Recinella
anr6832@rit.edu

Enhanced Flow Boiling Heat Transfer in Radial Microchannel and Offset Strip Fin Geometries

by

Alyssa Recinella

A Thesis Submitted in Partial Fulfillment of the Requirements for the Degree of Master of Science in Mechanical Engineering

Approved By:

Dr. Satish G. Kandlikar
Department of Mechanical Engineering _____
(Thesis Advisor)

Dr. Risa Robinson
Department of Mechanical Engineering _____
(Examiner)

Dr. Alfonso Fuentes-Aznar
Department of Mechanical Engineering _____
(Examiner)

Dr. Agamemnon Crassidis
Department of Mechanical Engineering _____
(Department Representative)

Rochester Institute of Technology

Rochester, New York 14623

November 2016

Enhanced Flow Boiling Heat Transfer in Radial Microchannel and Offset Strip Fin Geometries

by

Alyssa Recinella

A Thesis Submitted in Partial Fulfillment of the Requirements for the Degree of Master of Science in Mechanical Engineering

Department of Mechanical Engineering
Kate Gleason College of Engineering

Rochester Institute of Technology

Rochester, New York 14623

November 2016

Acknowledgements

Firstly, I would like to thank Dr. Satish Kandlikar for hiring me as a co-op student in 2014. Before joining the lab, my path as a mechanical engineer alluded me. Because of the 8 month co-op that I was fortunate to have, I fell in love with the subject and the research. His support and constant guidance has gotten me where I am today and I'm incredibly thankful. Thank you for giving me a chance.

This thesis would not have been possible without the efforts and help of Rob Kraynik, Jan Maneti, Craig Piccarreto, Bill Finch and countless others in the ME machine shop that have taught me how to machine and how to design. Their help and assistance has gone a long way. Another thank you to Diane Selleck, Jill Ehmann, Hillary McCormick and many others in the ME department for constantly brightening up my day and assisting in the advisement of my career. There are simply too many professors and faculty members in the department that have impacted my life in a positive way. Thank you for your constant encouragement.

Thank you to my committee members who have served not only to assist in the realization of this thesis but who have also given thoughtful and constructive feedback for this work. The insights provided by Dr. Risa Robinson, Dr. Alfonso Fuentes-Aznar and Dr. Agamennon Crassidis have helped this work greatly and I appreciate it.

I would also like to thank my fellow lab members, past and present, who have not only assisted in my engineering development but who have also selflessly given up time and resources to aide in my research. A big thank you to Ankit Kalani, Arvind Jaikumar, Pruthvik Raghupathi and Brittany Klimtzak for their loving friendship in and outside of the lab. Thank you to my friends that have provided love and laughter; David Schwartz, Matthew Wong, Avanell Brock, Rachel

Adams, Rachael Socolof, Robert Kelley, Joanna Robinson, Emily Becker, Clay Benson and many more.

Thank you to the organizations I'm a part of and all of the loving people in them. Most notably Flower City Pickers, Engineers for a Sustainable World, Intervarsity Christian Fellowship and Northridge Church. Without the love and support from these organizations, my sanity probably would have faltered. Thank you for being a family in a city that was unfamiliar.

And last but not least, thank you to my incredibly supportive and loving family. Cara and Trevor, thank you for believing in me and giving me the strength and humor to continue on from a Bachelor's degree to a Master's degree and to an eventual PhD. Thank you to my beautiful parents who have supported and nurtured my engineering habits from a young age from jigsaw puzzles to Rubik's cubes to calculus books. Mom, thank you for passing down your creativity and optimism. Dad, thank you for the "engineering gene" and helping me with your own engineering experiences. You have all supported me mentally, religiously, emotionally, and financially my entire life and I cannot even begin to describe my gratitude. This one is for you.

Abstract

Devices used for various electronic purposes are increasing in power consumption and performance. Due to this growth, the amount of heat dissipated over a small surface area has proportionally continued to increase. Despite previous efforts involving single phase natural and forced convection, these methods are no longer effective in high heat removal. Research in two-phase liquid cooling has become more prominent. Boiling has the potential to yield large critical heat flux values, high heat transfer coefficients and lower pressure drops. Many different surface enhancements and working fluids have been tested to increase efficiency and minimize heat losses.

Flow boiling in microchannels have been widely explored in literature for high heat flux dissipation. Microchannels are compact and subsequently easy to manufacture. However, due to flow instabilities that accompany microchannels, different configurations and additional modifications have been explored in order to maximize performance. In this work, a radial geometry is experimentally investigated with a flow inlet over the center of the chip. This central inlet creates a reduction in flow length and therefore a reduction in pressure drop and flow instabilities. Two testing surfaces were explored including a radial microchannel array and a radial offset strip fin array. To maximize performance even further, a gap has been added between the cover plate and testing surface to increase flow area and reduce pressure drop. One significant observation shows that an increase in flow rate mitigates the instabilities seen in the channels and prolongs critical heat flux (CHF). Due to these phenomena, all configurations are tested in the modified configuration with higher flow rates ranging from 120-320 mL/min.

Radial microchannels with an added gap yielded maximum performance values of 385.5 W/cm^2 at 42.7°C wall superheat with a high pressure drop of about 140 kPa while the offset strip

fin configuration achieved much higher heat transfer performance with CHF values exceeding 900 W/cm^2 at 58.6°C wall superheat. The offset strip fin geometry shows significant performance enhancements compared to the microchannels. For both the gap geometries and the closed geometries, the offset values are much higher than the radial microchannels.

Table of Contents

List of Figures

List of Tables

Nomenclature

Heat flux per unit area	q''
Wall temperature	T_{wall}
Saturation temperature of water	T_{sat}
Chip temperature	T_c
Thermal conductivity of copper	k_{Cu}
Distance between thermocouples	x

Chapter 1: Introduction and Background

In the world of electronics, heat is always a byproduct. In order to ensure reliability and to prevent any damage to electronic systems, this heat must be removed. Previous methods of cooling focused primarily on air cooled systems and recently on single-phase liquid cooling. However, due to the miniaturization of electronics that yield higher performance and require an increase in power, there is a growing need for advanced cooling techniques. Over the past decade, research in two-phase liquid cooling has risen in popularity. Because of latent heat effects, boiling has the ability to dissipate vast amounts of heat. The heat transfer coefficient in two-phase cooling is vastly larger compared to the heat transfer coefficient in single-phase cooling. A comparison of heat transfer coefficients of various cooling techniques can be seen in Table 1.

Table 1. Typical values of convection heat transfer coefficient.

Process	**Fluid**	**Heat Transfer Coefficient (W/m^2K)**
Natural Convection	Gases	2 – 25
	Liquids	50 – 1000
Forced Convection	Gases	25 – 250
	Liquids	100 – 20,000
Flow Boiling	Liquids	5,000 – 100,000

Compared with other cooling methods, boiling has a higher ability of dissipating large amounts of heat. Throughout literature, flow boiling has consistently shown great promise in cooling high-powered systems that generate a lot of heat. Several phases of flow boiling can be experimentally observed through various enhanced surfaces including microchannels. A deeper understanding of the boiling curve can assist in quantifying collected results.

1.1 Flow Boiling

Similar to the pool boiling curve, the flow boiling curve has multiple descriptive stages beginning with single phase convection and ending at film boiling. The main difference between the flow and pool boiling curves is the addition of a mass flux. While pool boiling remains stagnant, flow boiling is propelling a constant force across a heat surface. The flow boiling curve accounts for this force and creates a curve dependent on the tested mass flux.

The boiling curve, seen in Figure 1**,** shows wall superheat on the x-axis and heat flux on the y-axis. The wall superheat is calculated by subtracting the liquid saturation temperature from the wall temperature while the heat flux is the amount of heat dissipated per unit area over the tested surface. Each region of the plot signifies specific different boiling regimes. These regimes were first identified by Nukiyama [1] in a pool boiling system and are described below.

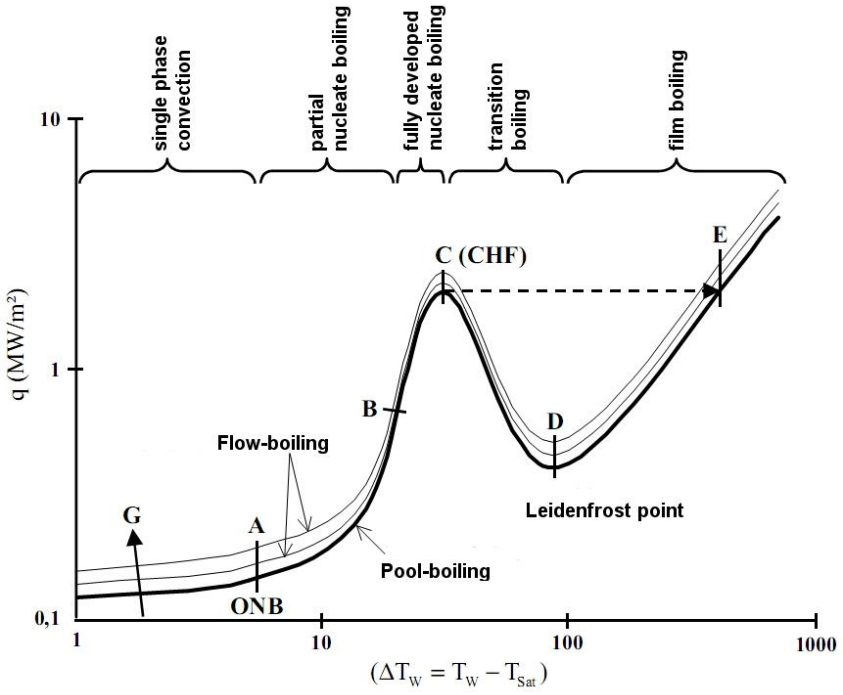

Figure 1. Flow boiling curve [2]

1.1.1 Single Phase Convection

In this phase, the temperature of the surface is greater than the temperature of the water. Heat is transferred from the hot surface into the water through free convection. No boiling occurs in this region until onset nucleate boiling, which can be observed in Fig. 1 (point A).

1.1.2 Nucleate Boiling

This region is generally split into two regions; partial nucleate boiling and fully developed nucleate boiling. During this process, bubbles form in the microscopic cavities found in the surface and slowly start to grow. Eventually the nucleated bubbles depart the surface and are swept away with the ongoing current. This process increases the heat transfer coefficient and the amount of heat dissipated over the heated surface, or heat flux. At point B, seen in Fig. 1, the heat transfer coefficient reaches its maximum. It is also at this point that rapid nucleation begins. Bubbles will nucleate at a quicker rate, forming columns or jets of continuous bubbles. It is at this point that the rate of bubble growth is faster than fluid velocity and the bubbles begin to coalesce. The coalesced bubbles form a massive layer of vapor over the heated surface and prevent any liquid from cooling down the surface. This phenomenon is called critical heat flux (CHF) and it can cause a significant amount of damage to the chip or setup that is being tested. CHF is seen at point C in Fig. 1.

In most flow boiling systems, when CHF is finally reached at point C, the curve jumps to point E (seen on the plot) and enters into film boiling. This dramatic increase in surface temperature causes a system meltdown and subsequently a sharp reduction in thermal performance.

1.1.3 Transition Boiling

Transition boiling signifies the region between nucleate and film boiling. Due to a consistent layer of vapor over the surface and continuous fluid flow on top of the vapor, the heat flux slowly begins to decrease. The formed film creates an insulated effect and prevents the rapid dissipation of heat observed in the previous region. The physical conditions at this point oscillate between film and nucleate boiling with a constant cycle of film growth and collapse.

1.1.4 Film Boiling

The Leidenfrost point (point D in Fig. 1) is when the heat flux reaches its lowest point. The film layer completely covers the surface and all occurring heat transfer occurs by conduction from the surface, through the film, to the liquid. As the surface temperature increases, the heat flux begins to increase as well.

1.2 Flow Regimes

Different flow regimes are used to identify the phenomenon appearing throughout the flow boiling process. The way the bubbles change can provide significant insight into the underlying mechanism happening over the span of the experiment. The following flow regimes were identified in microchannel flow boiling by Harirchian and Garimella [3] and can be visually observed in Fig. 2. The microchannels used for the experiment were 400 μm x 400 μm.

Bubbly flow is the first stage of boiling experienced in the channels. This phase occurs at the beginning of nucleate boiling when the nucleation rate is slower than the flow velocity. The bubbles are formed, grow, detach and are swept through the channels. Bubbly flow can be seen in the first frame in Fig. 2.

The second frame shows the beginning of slug flow. At this point, the boiling rate begins to speed up and the amount of detached bubbles is rapidly increasing. The flow velocity can no longer remove individual bubbles and instead, these nucleated bubbles begin to coalesce. The longer streams of vapor, known as slugs, can occupy the entire channel and produce instability and back flow. The third frame shows a choppier and more chaotic version of slug flow with rapid nucleation occurring.

Annular flow, observed in the fourth and fifth frames, arises when the vapor level caused by rapid nucleation forms a constant stream of vapor surrounded by the liquid flow.

The sixth frame, indicating inverted annular flow, shows a vapor blanket formed by the rapid nucleation rate which eventually starts to cover the channels preventing liquid from reaching the surface. It is at this stage that critical heat flux is reached and meltdown can start to occur.

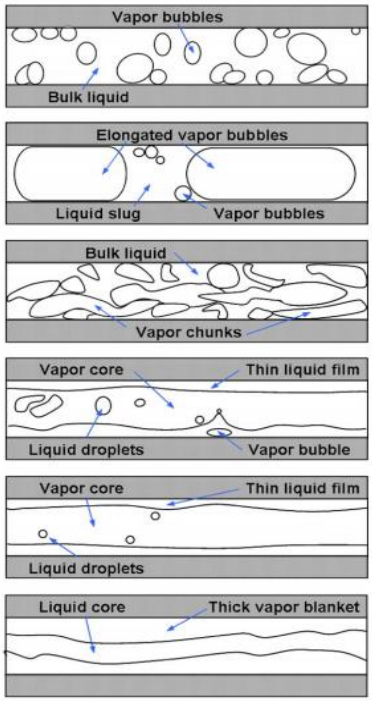

Figure 2. Varying flow regimes observed in rectangular, parallel microchannels. [3]

1.3 Surface Enhancements

In order to obtain optimum heat transfer performance, different parameters have been changed including working fluid, materials used for cooling and the addition of different surface enhancements. Various surface enhancements have been explored throughout literature including microporous structures, nanostructures and microchannels. The surface enhancement technique used in this study is microchannels. The classification of different channel structures was determined by Kandlikar and Grande [4]. The criteria used for specific classification is based on the channel hydraulic diameter or the diameter of the channel that is in contact with the working fluid. The hydraulic diameter of microchannels ranges from 10 μm to 200 μm.

Microchannels have produced good results for dissipating a large amount of heat over a small surface area. The simple design of the geometry has been used for a wide array of applications and the channels themselves are easily fabricated. Many different patterns and dimensions have been tested including straight, rectangular microchannels [5,6], pin fins [7,8], and a wide array of differently shaped channels [9–12].

1.4 Instability

Despite the rapidly growing microchannel trend, there are still problems to overcome. Many researchers that study flow boiling through microchannels have seen common instability trends ranging from inconsistent results to flow reversal and back flow. Numerous reasons have been mentioned including channel length and system geometry, lack of setup feasibility, and rapid bubble growth [13,14].

A significant factor of instability observed in nucleating channels is rapid bubble growth and backflow. While heat is added and bubbles begin to nucleate in the tested channel, pressure

fluctuations can be observed. This fluctuation can cause the pressure experienced at the nucleating bubble to spike and become larger than the initial pressure seen at the liquid inlet. The built up energy experienced in the nucleating bubble will eventually cause the bubble to grow and depart. However, with an internal higher pressure, the bubble begins to expand in both directions until the bubble pressure is lower than the liquid inlet pressure. It is at this point that the remaining vapor is swept downstream until the process begins again. This pressure fluctuation is experience for all bubbles nucleating in the channel and can create a significant amount of backflow and instabilities. A representation of this phenomena can be seen in Fig. 3 [15].

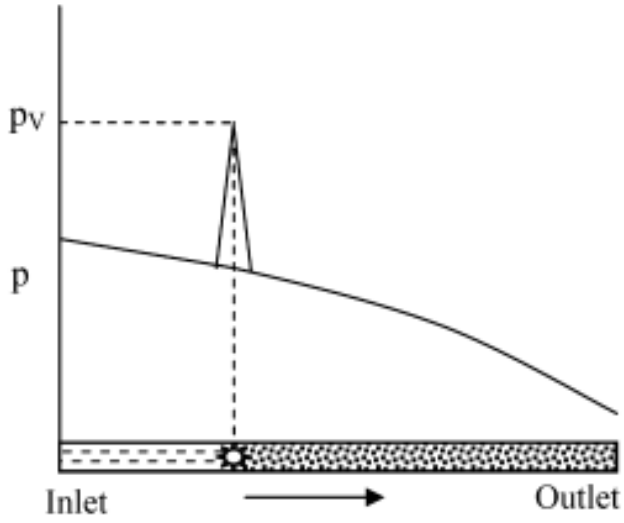

Figure 3. Observable pressure variations during bubble nucleation [15].

Chapter 2: Literature Review

Flow boiling heat transfer has multiple advantages which include high heat transfer coefficients, low coolant inventory and higher critical heat flux values. However, flow instability has shown to severely affect its thermal performance. The literature review section focuses on the techniques used by different researchers to further enhance flow boiling heat transfer and overcome the above mentioned issue. A variety of researchers have experimentally tested microchannels with several different working fluids and materials in order to overcome experimental shortcomings and augment the heat transfer performance of the testing surfaces.

2.1 Experimental Shortcomings

Different limitations including back flow, severe pressure drop and premature CHF have caused experimental issues in flow boiling and have been observed and recreated many times throughout literature. Back flow instability was observed by Qu and Mudawar [16]. They saw severe pressure drop oscillations as well as significant back flow of vapor into their inlet plenums. A possible cause for this instability could be in increase vapor generation colliding with a compressible volume upstream of the experimental test setup. Drastic instabilities such as pressure drop oscillations can cause premature critical heat flux. However, a vast majority of these oscillations were eliminated through the use of a throttling valve, directly upstream of the tested channels. Hetsroni et al. [17] observed a similar phenomenon; a vapor slug was pushed in both upstream and downstream directions, leading to a reversed flow. They also concluded that an increase in vapor quality will result in pressure drop amplitude fluctuations. Bergles et al. [18] observed oscillating flow and premature CHF. They determined that an enhanced wall friction presence, an additional pressure drop due to acceleration and internal compressibility in long

channels created these oscillations. Artificial nucleation sites [19] and inlet restrictors [16] were observed to stabilize flow.

2.2 Microchannels

Despite various experimental shortcomings, microchannels have been widely used in the electronics cooling industry due to their compact size, ease of fabrication and good thermal performance. Various researchers have attempted to vary the fin and channel patterns in order to enhance performance and yield greater results. Chu et al. [10] introduced curved rectangular microchannels. Niklas and Favre-Marinet [9] used triangular channels embedded in silicon. Deng at al. [6] compared straight microchannels to a unique Ω-shaped reentrant configuration and found that the new Ω-shaped geometry provided a significantly lower pressure drop than the rectangular channels. Other studies include diverging channels with added artificial nucleation sites by Lu and Pan [20] and stepped microchannels resulting in reduced flow instability were studied by Balasubramanian et al. [21]. Renaud et al. [22] performed a comparative study of silicon microchannels. The theoretical work created a 2D model based on the Navier-Stokes equations to describe flows in shallow microchannels. The experimental work simulated the flow characteristics in microfluidic devices utilizing microchannels in silicon. The theoretical model verified the experimental data. Daniels et al. [23] studied flow boiling through fractal-like microchannels under adiabatic conditions. A model for the pressure drop and vapor quality through the channels was developed and yielded good results. They concluded that the fractal flow networks are sensitive to the length ratio used but presented inconclusive findings for the exact desired length ratio that should be created. Xiao and Yu [24] created a numerical model simulating subcooled flow boiling based on the distribution of active nucleation sites. The fractal analysis performed was compared to experimental data and was verified. Another numerical study,

conducted by Chai et al. [12], includes a heat transfer model simulating trapezoidal silicon microchannels bounded to the same conditions seen in an experimental study. The numerical models displayed a faster velocity development and a consequential lower pressure drop. Favre-Marinet et al. [25] performed a comparative study investigating momentum and heat transfer in microchannels. Three separate investigations were conducted including a microchannel network study, a roughness study and a numerical model of heat transfer in channels. Overall, their results stress the importance of proper documentation and allowed for the future elimination of unwanted uncertainties in calculations.

2.3 Offset Strip Fins

Pin fin [7,26,28–32] or offset strip fin [33–39] configurations have been used by various researchers to enhance boiling performance. Offset strip fins provide a flow interruption which leads to heat transfer improvement through the creation of fresh boundary layers. Kim and Sohn [33] experimented with an offset strip fin flow boiling test setup using R113 as the working fluid. Vary mass fluxes ranging from 17 – 43 kg/m^{2}s achieved heat transfer coefficients between 700 – 3,000 W/m^{2}K. Pulvirenti et al. [34] explored vertical channels with offset strip fins using HFE-7100 as the working fluid. The convective boiling and nucleate boiling regimes were detected and local flow boiling heat transfer coefficients were measured between 4,000 – 10,000 W/m^{2}K.

2.4 Radial Microchannels

Similar to rectangular, parallel channels observed in literature, radial microchannels used in flow boiling are identical in width and depth and are designed for a similar purpose. The major fallback of straight microchannels is a higher pressure drop. With a radial array of channels and a central inlet, the area cooled by the working fluid is nearly cut in half. Because of this design,

theoretically the pressure drop through the channels is halved. Surfaces similar to this design, mainly fractal geometries, have been tested widely throughout literature. A number of theoretical [24, 25, 27] and numerical [25,41–44] studies have also been published based on flow boiling in radial microchannels.

Pence and Enfield [45] performed a comparative study between a fractal-like network and parallel channels. Using identical flow rates, power inputs and a supplied heat flux of 100 W/cm^2, they found that the total pressure drop in the fractal network was approximately 2.1 times higher and the wall temperature 27°C higher than parallel channels. A visual representation of the fractal network utilized for this study can be seen in Fig. 4.

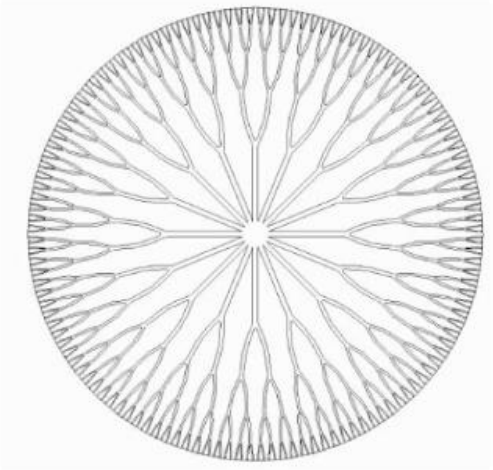

Figure 4. Fractal network used for an experimental flow boiling study [45].

Apreotesi et al. [46] studied a similar fractal-like branching network of channels. When put into single-phase conditions using a subcooling temperature of 2.5 K and a flow rate of 8 g/min, they achieved a pressure drop of 0.9 kPa. Liburdy et al. [47] studied a fractal-like branching network embedded in silicon with hydraulic diameters ranging from 143 μm – 308 μm. Utilizing water at

an inlet temperature of 88°C with a high, constant flow rate, the study focused on experimentally comparing void fraction with and without the addition of a throttle valve. Results showed that there was significant flow reversal in the bifurcating channels, regardless of throttling. Daniels et al. [23] compared adiabatic boiling through fractal-like branching microchannels with numerical simulations. At large varying flow rates and subcooling temperatures from 0.5-6°C, they found that the pressure drop is significantly influenced by the inlet subcooling. Ruiz et al. [48] experimented with a radial boiling pattern on a plain copper chip and a chip coated in zinc oxide nanostructures. Using distilled water as the working fluid at a consistent mass flux of 184 kg/m^{2}s, an average heat flux of 169 W/cm^2 at an inlet temperature of 22°C was found for distilled water. On the ZnO coated surface at the same 184 kg/m^{2}s mass flux, a higher heat flux of 196 W/cm^2 was found. As the mass flux was increased, the maximum heat flux steadily increased as well. The study concluded that added microchannels would enhance critical heat flux values by as much as 16%. The setup they used can be observed in Fig. 5.

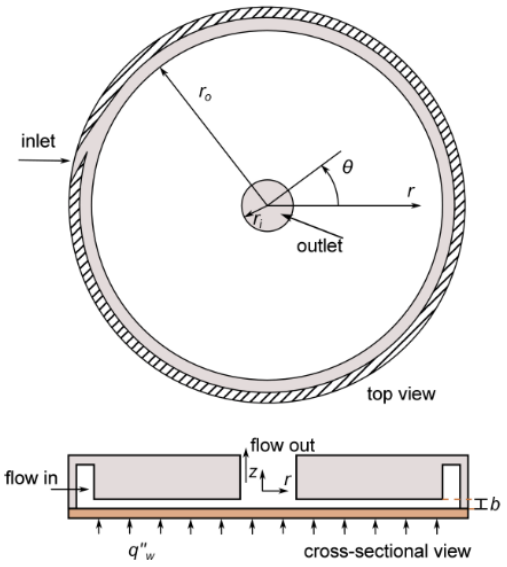

Figure 5. Radial inlet/outlet manifold on a plain copper surface [48].

Shultz et al. [49] experimented with a radial array of channels using dielectric coolant R1234ze. The coolant is injected in the center, spreads through the radial array of channels and exits at the edges of the testing surface. Despite various flow instabilities and channel blockages, they were able to dissipate approximately 350 W/cm^2 with a flow rate of 15 kg/hr and a stable pressure drop of 320 kPa. A schematic of the chip and setup used for testing can be seen in Fig. 6 (a) and (b).

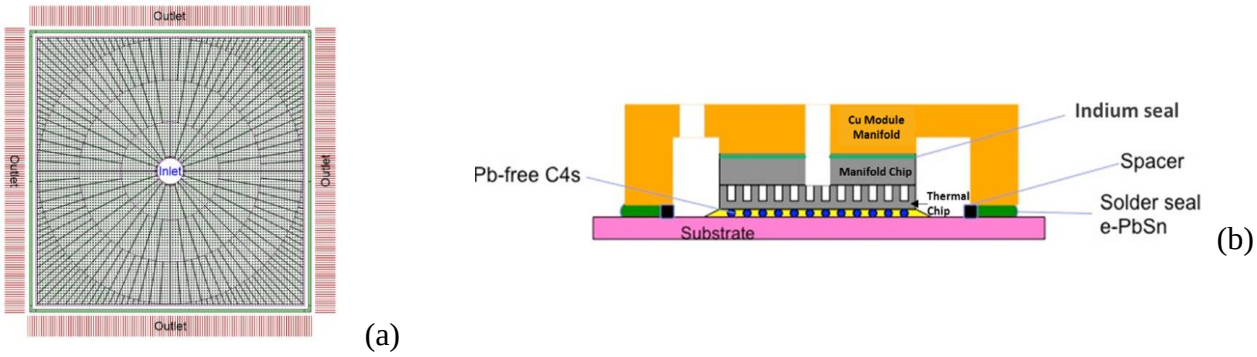

Figure 6. (a) Radial microchannels embedded in silicon (top view) and (b) setup used for boiling tests.

Further improvements for performance enhancement involve modifications to the cover plate. Kalani and Kandlikar [50] introduced open microchannels with the addition of a gap and a tapered manifold (OMM) on straight channels. The gap and taper add extra area for the water to flow while also providing space for nucleating bubbles to depart before massive bubble coalescence. This study saw drastic improvements in heat transfer performance with a reduction in pressure drop. The heat transfer performance increased from a heat flux of 227 W/cm^2 at a wall superheat of 22 °C to a heat flux of 283 W/cm^2 at 12 °C wall superheat. The pressure drop reduced from a maximum 62 kPa to 3 kPa. These results show favorable results for future studies and a schematic of the cover plate used can be seen in Fig. 7.

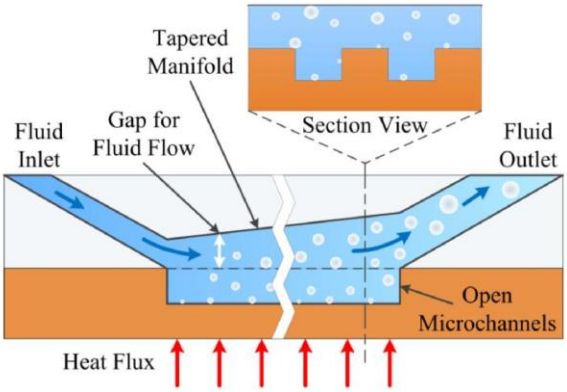

Figure 7. Open microchannels with tapered manifold [50].

2.5 Scope of Work

Despite various surface enhancements positively altering the heat transfer performance, pressure drop and flow instabilities during boiling, further modifications are needed for proper performance. This study focuses on an experimental investigation of radial microchannel and radial offset strip fin geometries. Theoretically, the reduction in flow length should yield lower pressure drop and increase heat transfer performance.

Based on the pioneering work of London and Shah [38] and Carey and Mandrusiak [37], offset strip fins show great promise in further performance enhancements. The strip fin geometry provides a flow disruption and creates turbulent flow in the single phase boiling regime. Arranging offset strip fins in a radial pattern creates an opportunity for similar heat transfer performance enhancements while keeping the consistent theoretical pressure drop reduction associated with the radial configuration.

Similar to the work presented by Kalani and Kandlikar [50], an added gap and taper create an open microchannel configuration (OMM), allowing for a larger flow area. The increase in space

lets nucleating bubbles to float towards the manifold instead of lingering in the microchannels. This can prevent rapid bubble growth leading to vapor blanketing and eventual critical heat flux.

This study focuses on combining all of these components for maximum heat transfer performance with low pressure drop. A radial flow configuration, offset strip fins and an added gap creating an open microchannel geometry are all explored below.

Chapter 3: Experimental Work

3.1 Flow Loop

Figure 8 shows an overview of the test loop used in the study of flow boiling with radial microchannels. The test loop, based on previous works [51], consisted of a pressure cooker on top of a hot plate which acted as a liquid reservoir and degassing unit. The working fluid (distilled water) is degassed before every test to remove any non-condensable gases [13]. The high temperature fluid flows through a shell-in-tube heat exchanger in order to cool the water before it arrives at the Micropump©. This prevents any overheating of the pump that may occur. A rotameter is used to control the flow rate while inline heaters were used to control the temperature of the water as it entered the test section. An inlet subcooling of 15°C was maintained for all test runs. The flow rates used in this study ranged from 120 mL/min – 400 mL/min for the first configuration and 120 mL/min – 320 mL/min for the second.

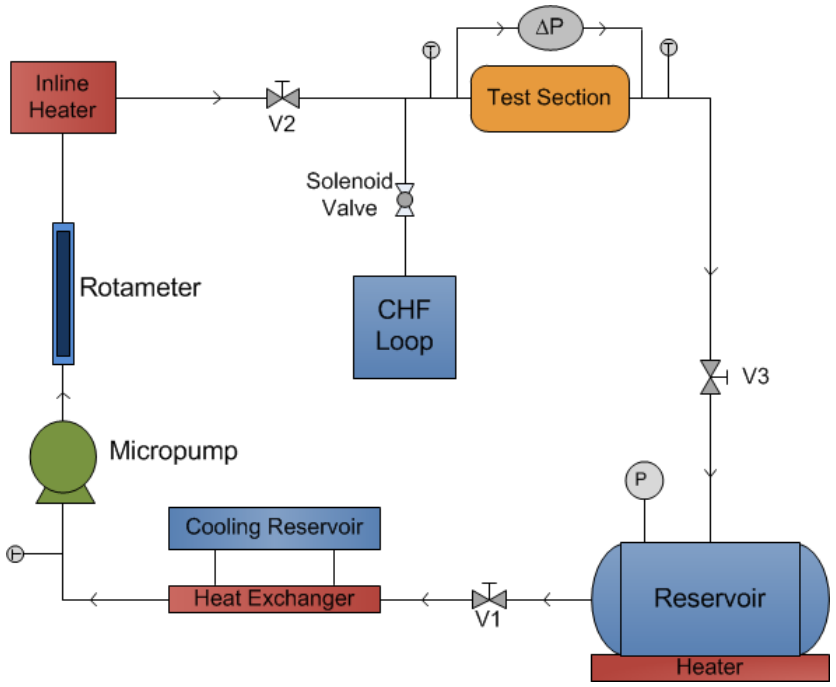

Figure 8. Schematic of flow boiling test loop.

3.2 *Test Setup*

The test setup used for experimentation involves a copper heater, described in further detail below, sandwiched in between two aluminum plates and additional hardware to ensure the top surface sits flat. The copper heater is surrounded with various pieces of ceramic insulation to reduce heat losses. Holes are placed strategically throughout the block for cartridge heaters and thermocouples. Finally, a polysulfone manifold rests on top in contact with the copper surface. Silicone gaskets and aluminum shims are added in order to incorporate changing testing parameters such as a gap. This test setup can be seen in Fig. 9.

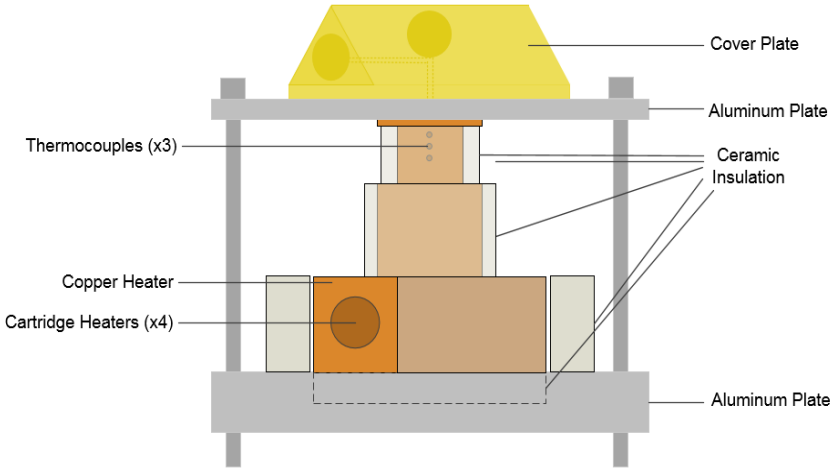

Figure 9. Test section (side view) used for experimentation.

3.3 *Test Section*

The flow loop and experimental section used for study can be observed below. The same copper heater was used for all experiments while the microchannel geometries varied for each test. Two separate manifolds were tested and many design changes were made throughout the entirety of this work. All configurations can be seen below.

3.3.1 Copper Heater

The test setup is comprised of a heated section seen in Figure 10. Four 400 W, 120 V Watlow© cartridge heaters are inserted into each side of the copper base. There are three thermocouple holes towards the top of the test section which are used to measure the temperature gradient and calculate heat flux. A backwards Taylor's series derivation is used to calculate the temperature gradient dT/dx:

$$\frac{dT}{dx} = \frac{3T_1 - 4T_2 + T_3}{2\,\Delta\, x}$$

where T_1, T_2 *and* T_3 are the three thermocouples observed in Figure 10 and x is the distance in between the thermocouples. Using this temperature gradient, the heat flux is calculated using one-dimensional conduction:

$$q" = -k_{Cu}\frac{dT}{dx}$$

The wall superheat is calculated using the following:

$$\Delta\, T = T_c - q"\left(\frac{x_1}{k_{Cu}}\right)$$

where T_c is the temperature of the heated surface, q" is the calculated heat flux, x_1 is the distance of the thermocouple to the heated surface (x_1 = 1.5 mm) and k_{Cu} is the thermal conductivity of copper.

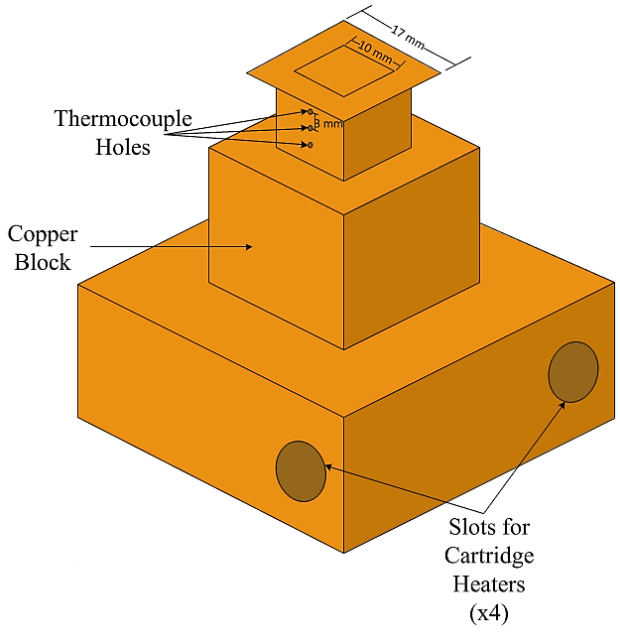

Figure 10. Schematic of the copper heater test section.

3.3.2 Test Surface

Two different surfaces were used for testing; radial microchannels and radial offset strip fins. The microchannel surfaces used for experimentation can be seen in Figures 11a and 11b. Figure 2a shows the radial microchannel array while Figure 2b shows the radial offset strip fin configuration. The radial fins are 200 µm in width and depth. The microchannel widths range from 200-700 µm. The central inlet for both geometries is 1.5 mm.

The offset strip fin configuration similarly has a 2 mm inlet. The fins are 200 µm in width, 200 µm in depth and 350 µm in length. The pattern created by the offset strip fins is slightly random. A minimum distance of 200 µm between fins was maintained for manufacturing purposes.

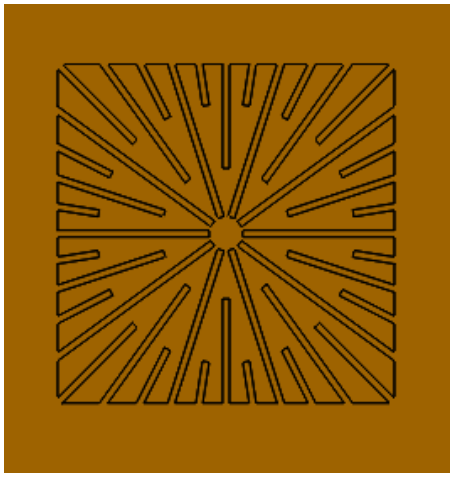

(a)

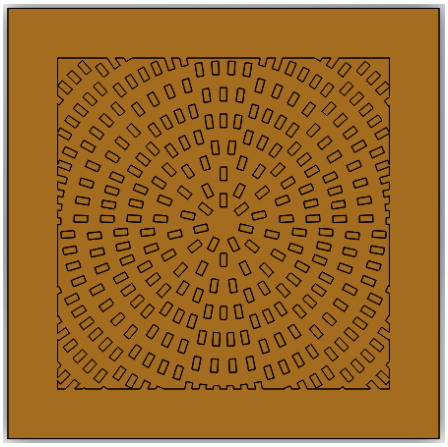

(b)

Figure 11. Schematic (top view) of the test surface (a) radial microchannels and (b) offset strip fins.

3.3.3 Original Manifold (Manifold 1)

The manifold assembly used for this study can be seen in Fig 12. The two blocks (one blue, one yellow) are a Lexan and Polysulfone block, respectively. The Lexan block provides both the inlet and outlets for the system. The inlet empties directly in the center of the radial array. At the outlet, the water is pushed through four separate slots in manifold block 2, collected in the in manifold block 1 and then exits through Swagelok tube fittings. The Polysulfone block was placed underneath the Lexan block and in contact with the copper surface due to its high glass transition

temperature of 140°C. A gasket between the two manifold blocks was provided for sealing purposes. However, this does not alter the performance or collected data.

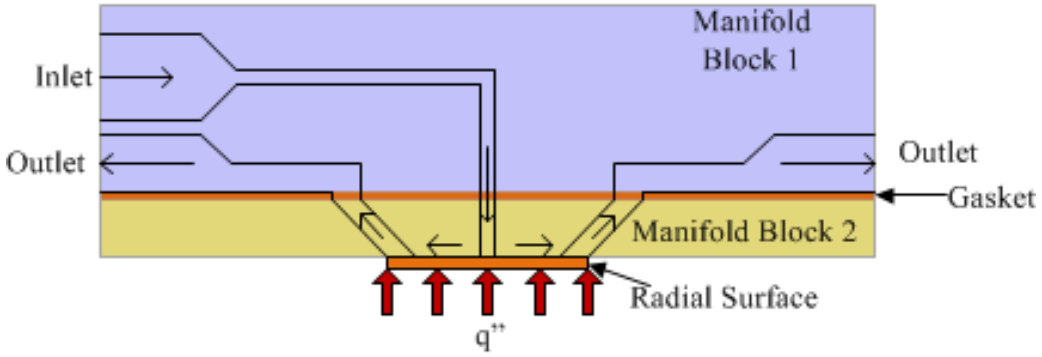

Figure 12. Cross-sectional view of the manifold assembly showing the manifold blocks and the test surface.

3.3.4 New Manifold (Manifold 2)

The cover plate used for study can be observed in Fig. 13. Dissimilar from the previous manifold, this manifold has one central inlet with four outlets on each side. The central inlet is 1.5 mm in diameter. The most significant difference between the two is that this block is made of one piece of plastic and is completely solid. Manifold 1 uses two separate pieces together to form the manifold whereas this manifold stands alone. The block is made of polysulfone due to the high glass transition temperature and the transparency of the material. Because the manifold comes in contact with the copper surface, a higher melting temperature is required to ensure sufficient testing is possible. The manifold also needed a certain level of transparency in order to incorporate high speed visualization during all testing. All configurations were tested over the same flow rate range from 120 – 320 mL/min with similar working conditions.

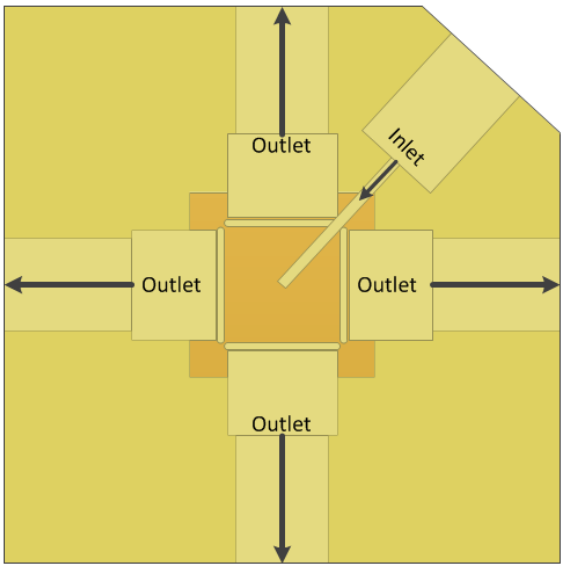

Figure 13. Schematic of the redesigned manifold block showing the inlet and outlets (x4).

a) Closed Microchannels

The first internal configuration between the manifold and the copper surface can be seen in Fig. 14. The water comes into the inlet, goes directly into the channels and exits out the four inlets (two are pictured here).

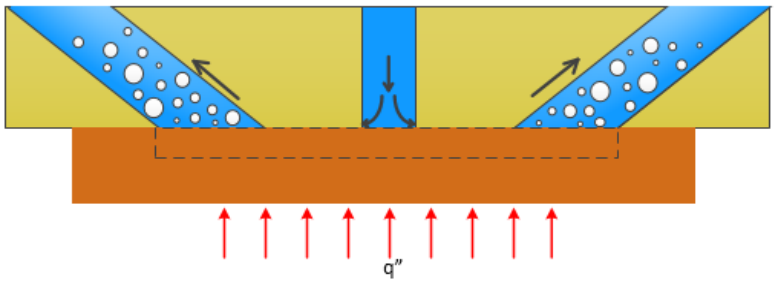

Figure 14. Closed microchannel configuration (side view) with central inlet and outlets (x4).

b) Open Microchannels

The second internal configuration involved a gap between the two surfaces. The gap was created with a metallic shim and a silicone gasket for sealing purposes. The added gap allows more area for liquid flow and subsequently a reduction in pressure drop. This configuration can be seen in Fig. 15.

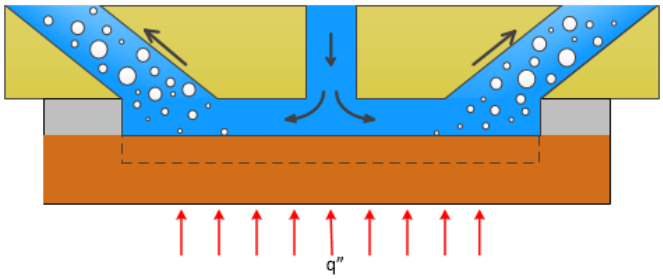

Figure 15. Open microchannel configuration (side view) with central inlet and outlets (x4).

c) Countersink

The third internal configuration tested included a countersink right at the inlet. The goal of the added countersink was to reduce the head loss in the system for a reduction in pressure drop. A gap is also added to create open microchannels as opposed to closed. This configuration is seen in Fig. 16.

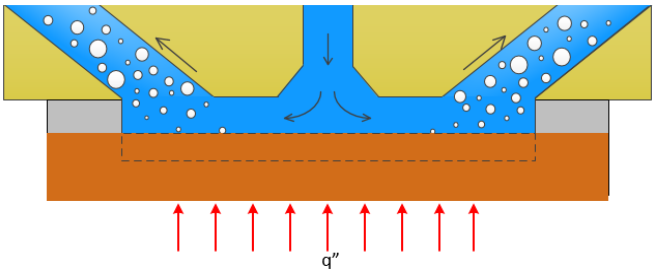

Figure 16. Open microchannel configuration (side view) with added countersink, central inlet and outlets (x4).

Chapter 4: Boiling Performance

This chapter focuses on the results obtained from all tests using both manifolds. The results for this study involve collected data from manifold one and manifold two, radial microchannels and radial offset strip fins, varying flow rates and an uncertainty analysis. The introduction of a gap and countersink between the second manifold and copper test surface was also explored. Water was used as the working fluid for all test runs and the tested flow rate was varied from 120 ml/min – 400 ml/min. The heat transfer performance are represented in the form of boiling curves which show the heat flux as a function of the wall superheat. The heat flux was calculated using the projected area of the test surface (10 mm x 10 mm). The wall superheat was calculated as the difference between the wall temperature of the surface exposed to the liquid and the saturation temperature. The wall temperature for the current work was taken as the temperature at the top surface of each test surface. The pressure drop data was obtained using a differential pressure sensor and its results are represented in the form of pressure drop versus heat flux plots.

All tests were visualized with a Photron FastCAM at 3000 fps and visualization results are discussed later in this section.

4.1 Uncertainty Analysis

A brief uncertainty analysis, similar to the work and experimental setup implemented by Kalani and Kandlikar [52], was performed for the first manifold configuration for collected heat flux data and pressure drop data. In the heat flux uncertainty study, the largest error seen was in the thermocouples. Multiple error factors were taken into consideration including calibration and precision. The uncertainty observed was approximately 0.1 °C. The heat flux uncertainty reduced as the heat flux increased from about 9% to 7%.

In the pressure drop uncertainty analysis, the largest error appeared in the lower flow rates used while the higher flow rates portrayed much lower uncertainties. The uncertainties also decrease as the wall superheat and heat flux values increase. The largest uncertainty seen is 19% while the lowest is at 2%.

4.2 Manifold 1

The results for the first manifold tested, seen in Fig. 12, are presented below. The first manifold described in chapter 2 includes two separate pieces of plastic with a silicone gasket. Both radial geometries were tested (radial microchannels and radial offset strip fins) with six different flow rates ranging from 120 – 400 mL/min. Heat flux, wall superheat and pressure drop data was collected and is presented below. A table of all collected data is seen in Table 2.

Table 2. Experimental data collected for radial microchannels and offset strip fins for the first manifold configuration.

	Flow Rate	q"	ΔT	ΔP
Radial Microchannels	120	86.7	24.8	2.4
	160	121.3	28.2	2.9
	200	145.4	36.7	4.2
	240	103.6	24.9	4.8
	320	181.5	44.5	9.1
	400	267.5	49.7	16.0
	Flow Rate	q"	ΔT	ΔP
Offset Strip Fins	120	67.6	28.6	2.5
	160	124.7	28.1	3.6
	200	162.8	36.5	6.1
	240	106.1	16.7	4.8
	320	164.8	18.1	9.0
	400	306.6	24.3	18.9

4.1.1 Heat Flux

The comparative boiling performance of the six different flow rates tested on both the radial microchannel surface and offset strip fins with added uncertainty can be seen in Fig. 17 (a) and (b). For both radial and offset geometries, similar heat flux values (~ <150 W/cm^2) were obtained at low flow rates (120 – 200 mL/min). Improved heat transfer performance was observed at higher flow rates. Significantly higher wall superheat was obtained for the radial geometry compared to the offset strip fin geometry for flow rates > 240 mL/min.

Figure 18 shows a comparison between the performances of the two separate surfaces for four flow rates instead of six for clarity purposes. At the maximum flow rate tested of 400 mL/min, the radial channels yielded a heat flux of 267.5 W/cm^2 at 49.7°C wall superheat while the offset strip fins achieved a maximum heat flux of 306.6 W/cm^2. Overall, the offset strip fin surface had significantly better performance than the radial microchannels.

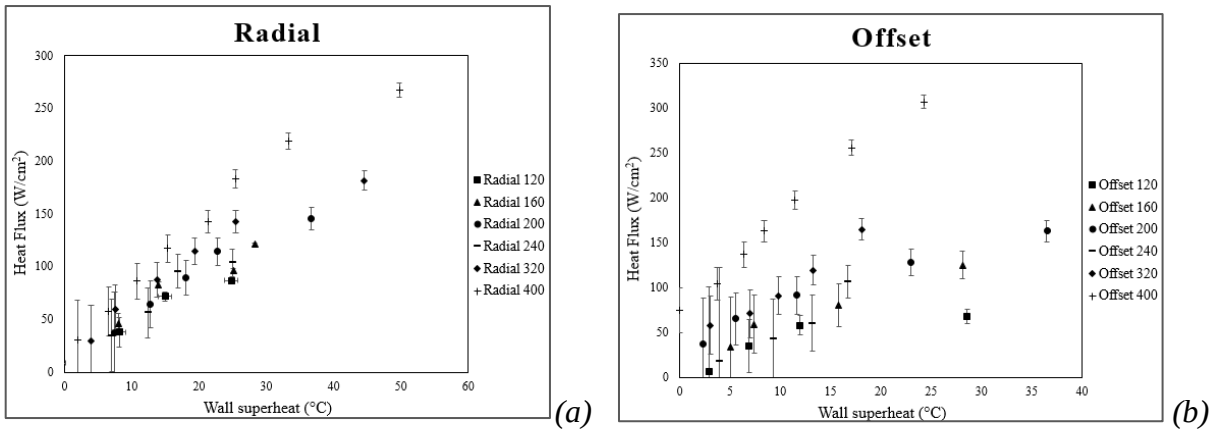

Figure 17. Heat flux vs. wall superheat for (a) radial microchannels and (b) radial offset strip fins.

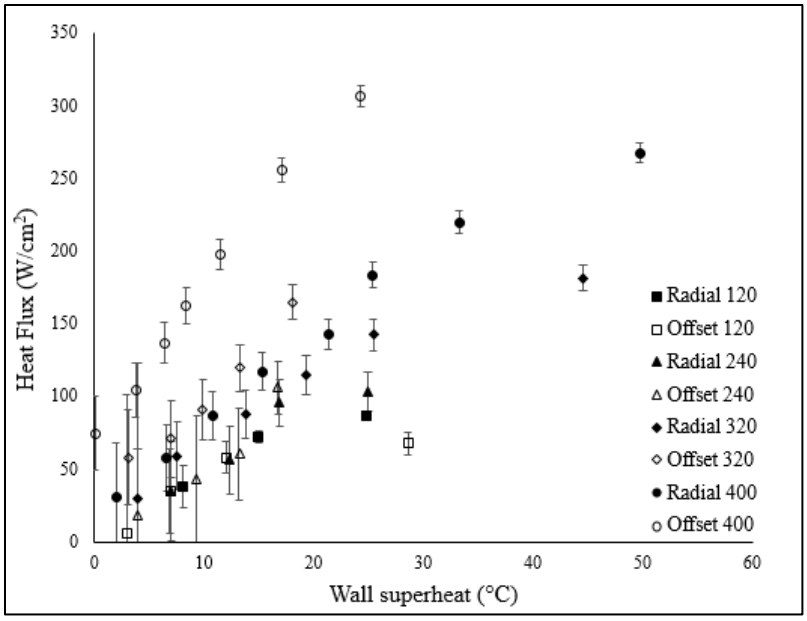

Figure 18. Comparative graph for calculated heat flux values for radial channels and offset strip fins; radial microchannels are in solid black and offset strip fins are hollow.

4.1.2 Pressure Drop

The pressure drop collected for each flow rate is presented in Fig. 19 (a) and (b) for both the radial microchannel surface and the offset strip fins with added uncertainty bars. For the radial and offset geometries, similar pressure drop values were seen at lower flow rates (120 – 240 mL/min) with an increase in pressure drop at higher flow rates (320 – 400 mL/min). Despite the increase in heat transfer performance with offset strip fins, the pressure drop stayed relatively consistent for both geometries.

Figure 20 shows the pressure drop comparison between the two surface geometries with radial microchannel data in solid black and offset strip fin data represented by the hollow symbols. For all flow rates, the radial channels increased from 2.4 kPa to 16 kPa while the offset strip fins increased from 2.5 to 18.9 kPa. Ultimately, the pressure drop did not change drastically between the two surface geometries.

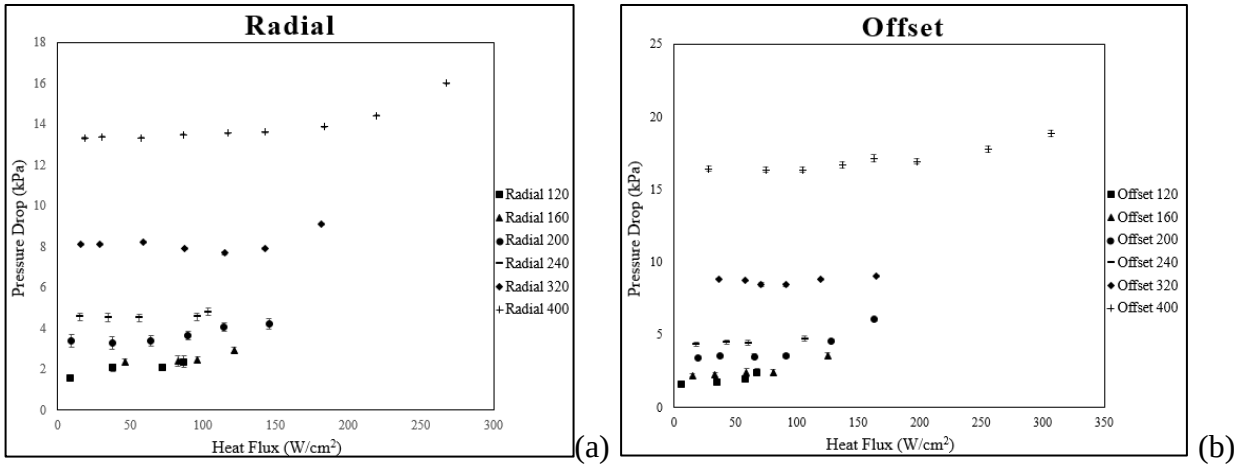

Figure 19. Pressure drop vs. heat flux for (a) radial microchannels and (b) radial offset strip fins.

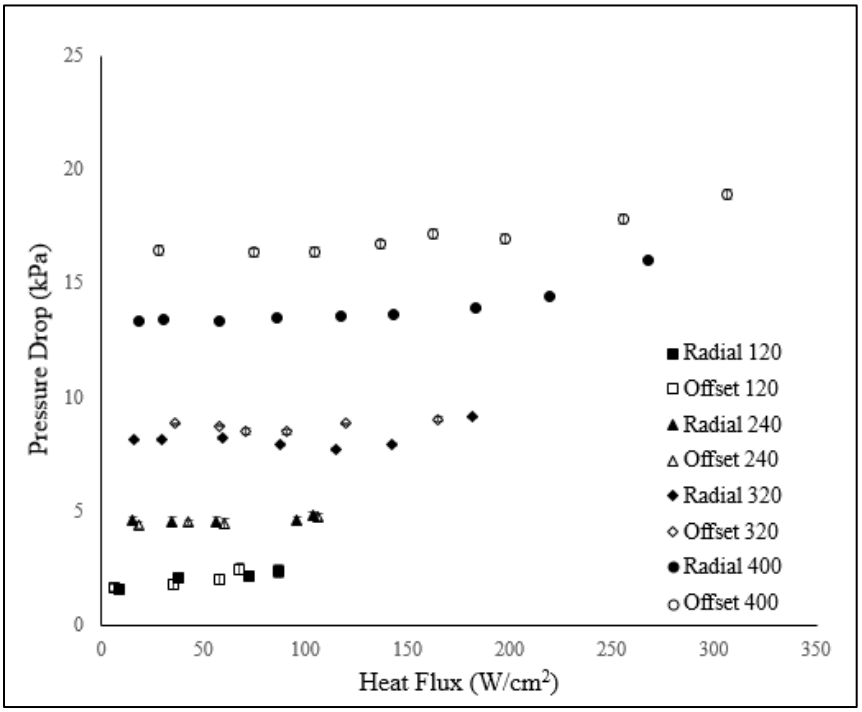

Figure 20. Comparative graph for measured pressure drop values for radial channels and offset strip fins; radial microchannels are in solid black and offset strip fins are hollow.

4.3 Manifold 2

The second manifold, observed in Fig. 13, had slightly modifications compared to manifold 1 including four outlets and one solid piece of plastic as opposed to two. Several different parameters were tested including flow rate, surface geometry, and inlet modifications. Heat flux and pressure drop values were collected and are presented below. A table of all collected data is seen in Table 3.

Table 3. Experimental data collected for radial microchannels and offset strip fins for the second manifold configuration.

	Configuration	Flow Rate	q"	ΔT	ΔP
Radial Microchannels	No Gap	120	237.5	27.5	38
		180	377.1	43.1	100
		240	352.9	30.1	110
		320	385.5	42.7	140
	Gap	120	348.3	48.8	28.9
		180	364.2	48.3	42
		240	368.8	48.7	59.4
	Configuration	Flow Rate	q"	ΔT	ΔP
Offset Strip Fins	No Gap	120	213.7	25.2	55
		180	479.3	32.7	145
		240	684.0	40.5	175
		320	904.5	58.6	190
	Gap	120	310.4	14.7	6.9
		180	483.6	16.8	7.2
		240	618.3	20.1	13.8
		320	897.2	63.7	190
	Gap and Countersink	320	976.2	51.3	210

4.3.1 Effect of Surface Geometry

Two different surface geometries were tested with the new manifold design; radial microchannels and offset strip fins. The varying heat transfer performance and pressure drop performance can be seen in Figures 21 and 22**,** respectively. At the higher flow rate of 240 mL/min with a closed microchannel configuration, the radial geometry yielded a heat flux of 502 W/cm^2 at a ΔT of 69°C and a pressure drop of 140 kPa. At the same flow rate and configuration, the offset strip fins showed a heat flux of 682 W/cm^2 at a ΔT of 40°C and a pressure drop of 175 kPa. The no gap configuration for both geometries yielded a higher maximum heat flux value compared with ones having gap. In literature, the work performed by Carey and Mandrusiak [37] using the offset strip fins has also yielded much better performance. During rapid boiling, the strip fins prevent massive bubble coalescence and therefore prolong boiling. This phenomena can be visualized and is explained below.

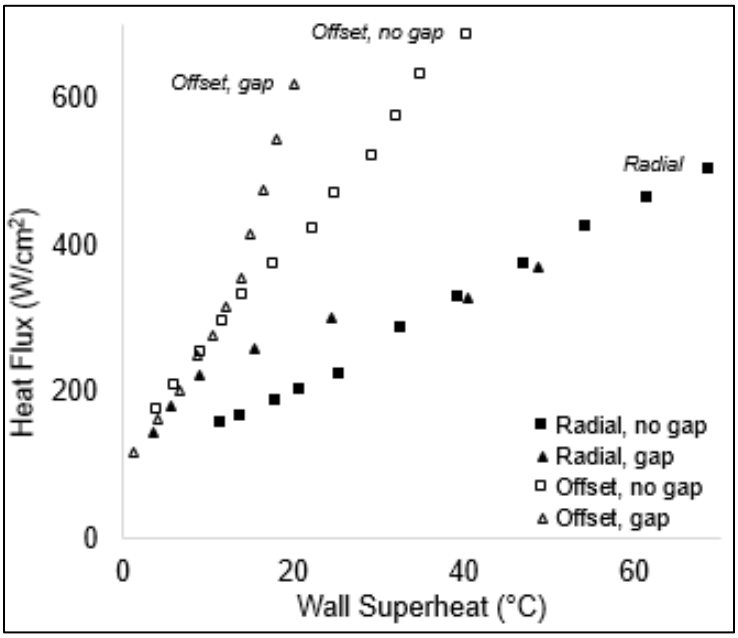

Figure 21. Effect of changing surface geometry where radial microchannels are in solid black and offset strip fins are hollow.

4.3.2 Effect of Gap

Similar to the study performed by Kalani and Kandlikar [50], a gap of 127 μm was added between the manifold and copper chip creating an open configuration. The performance was compared to the closed microchannel configuration. As expected, the pressure drop for both surface geometries reduced drastically. At a flow rate of 240 mL/min, the pressure drop for the radial microchannels dropped from 140 kPa to 59 kPa when critical heat flux while the offset strip fins reduced from 175 kPa to a mere 13.8 kPa. This phenomenon can be further observed in Fig. 22. The addition of a gap reduced the maximum wall superheat seen in the radial offset strip fins from 40.5°C in the closed geometry to 20.1°C in the open geometry. This reduction can be attributed to the added flow area created by the gap. The additional space allows the vapor bubbles to nucleate and evacuate the channels allowing for more water to flow. The added gap helps reduce the coalescence of vapor which can cause major instabilities and dryout.

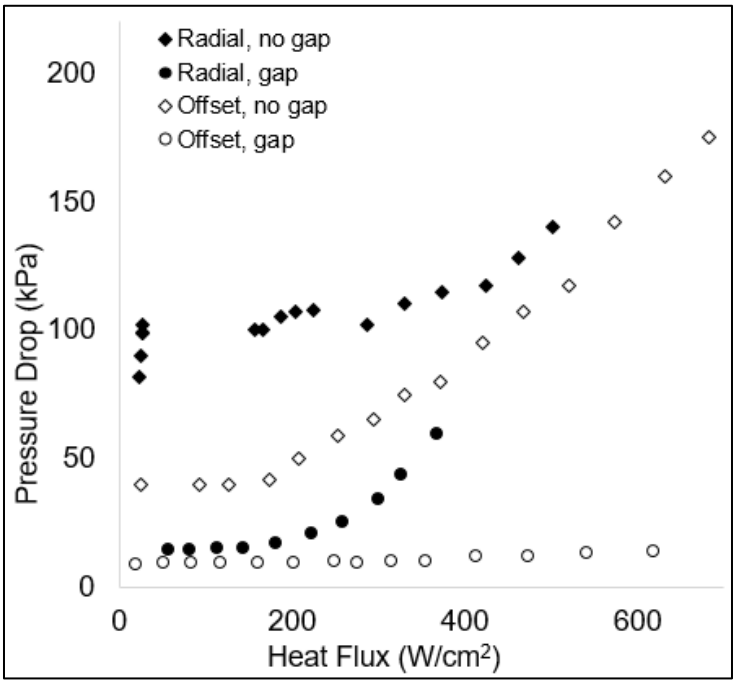

Figure 22. Effect of the added gap where radial microchannels are in solid black and offset strip fins are hollow.

4.3.3 Effect of Flow Rate

Four separate flow rates were tested using the second manifold geometry ranging from 120 – 320 mL/min. The results for the lowest flow rate (120 mL/min) and the highest (320 mL/min) can be seen in Fig. 23. Similar to the resulting phenomena seen using the first manifold, an increase in flow rate achieved reductions in flow instabilities and prolonged heat flux. Using the offset strip geometry at a flow rate of 120 mL/min, a maximum heat flux of 310.4 W/cm^2 was achieved at ΔT of 14.7°C while the higher flow rate of 320 mL/min had a q" of 897.2 W/cm^2 at ΔT of 63.7°C. Although there is an increase in wall superheat for higher flow rates, there is a drastic increase in highest achievable heat flux as well. These results are achieved using the second manifold, offset strip fin surface geometry and an open channel configuration.

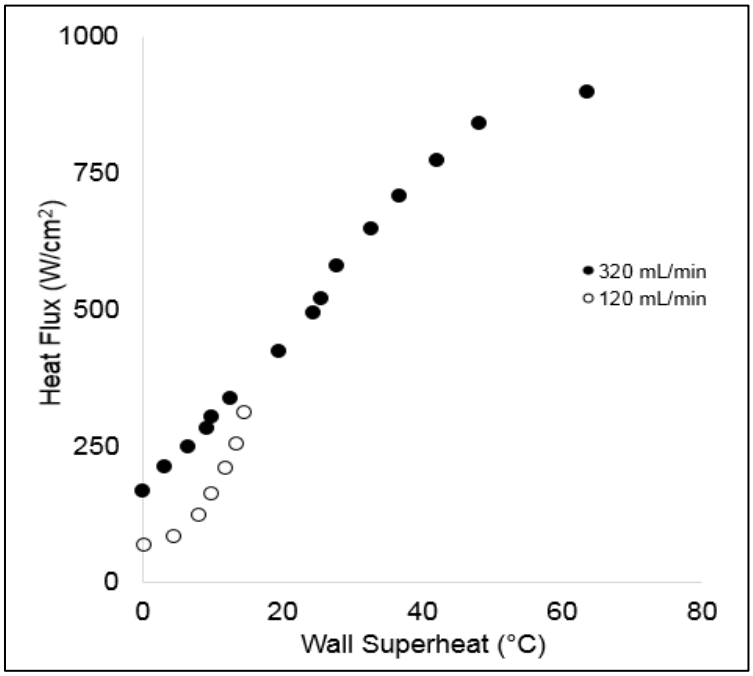

Figure 23. Effect of flow rate using offset strip fins.

4.3.4 Effect of Countersink

The final tested configuration involved the addition of a countersink at the inlet. The original intention of the addition was to reduce the pressure drop due to the head loss at the inlet (diameter of 1.5 mm) by adding a 45° countersink with a maximum diameter of ~3 mm. Due to the positive results obtained from offset strip fins, an open manifold configuration and the higher flow rate of 320 mL/min, only one test was performed with these attributes and the included countersink. Comparing the plain open configuration with the open, countersunk configuration, the initial pressure drop at the start of the test reduced from 55 kPa to 20 kPa, respectively. A maximum heat flux of 976 W/cm^2 was reached at a ΔT of 51.3°C. While the initial pressure drop was significantly reduced with the added countersink, the pressure drop at the maximum heat flux was ~210 kPa. This high value can be attributed to the rapid boiling occurring throughout the channels at a high mass flow rate. Further expansion of this countersink effect will yield very promising results. Results for pressure drop and heat flux can be seen in Fig. 24 and 25, respectively.

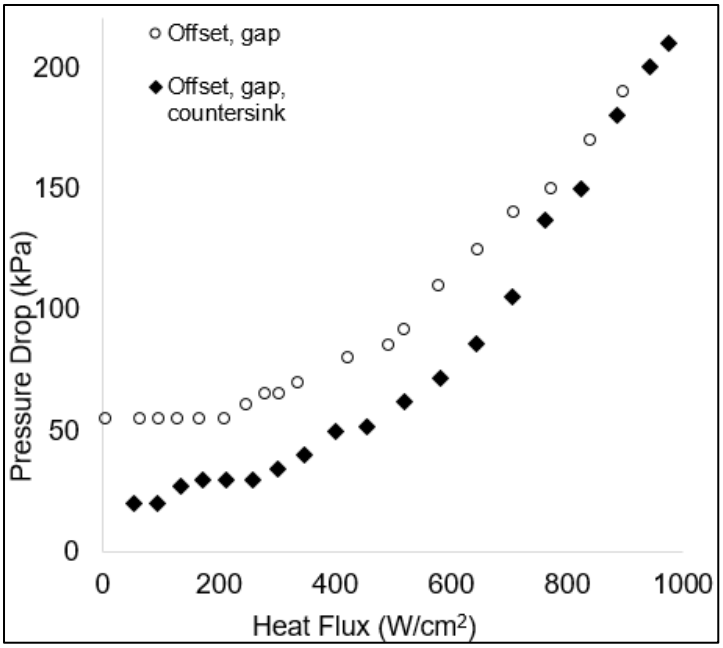

Figure 24. Comparative pressure drop of offset geometry with gap configuration and offset geometry with gap and countersink configuration.

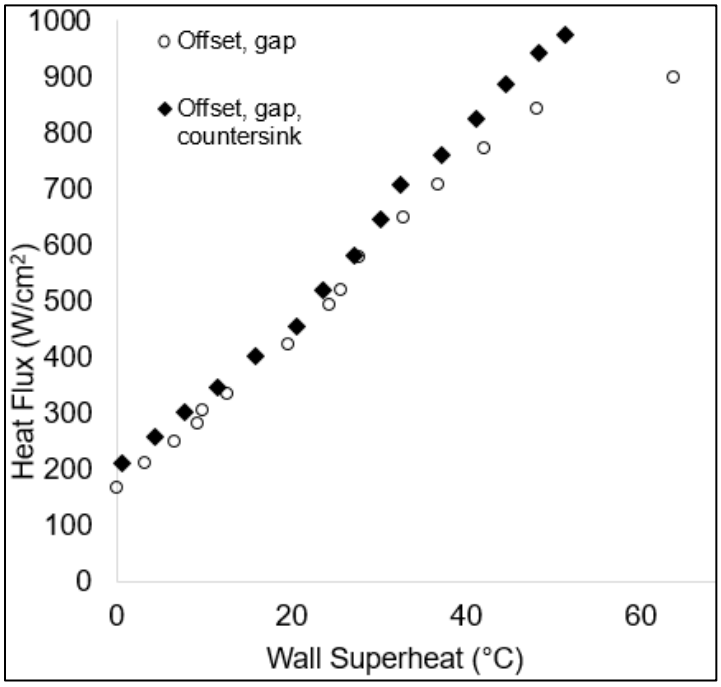

Figure 25. Comparative heat flux of offset geometry with gap configuration and offset geometry with gap and countersink configuration.

4.4 Visualization

A large part of this study involved the incorporation of visualization using a Photron FastCam at 3000 fps and a microscope light. Furthermore, the Photron FASTCAM Viewer software was used for image optimization.

4.4.1 Instabilities

The flow instabilities discussed above during testing of the first manifold can be visualized in Fig 26. The first frame shows a vapor/liquid mixture throughout the channels. The second frame shows that vapor/liquid mixture expanding and encompassing more channel area. Finally the third images has the mixture going backwards into the inlet as opposed to dispersing through the outlets. This is an example of the back-flow instabilities causing high pressure drops and early CHF.

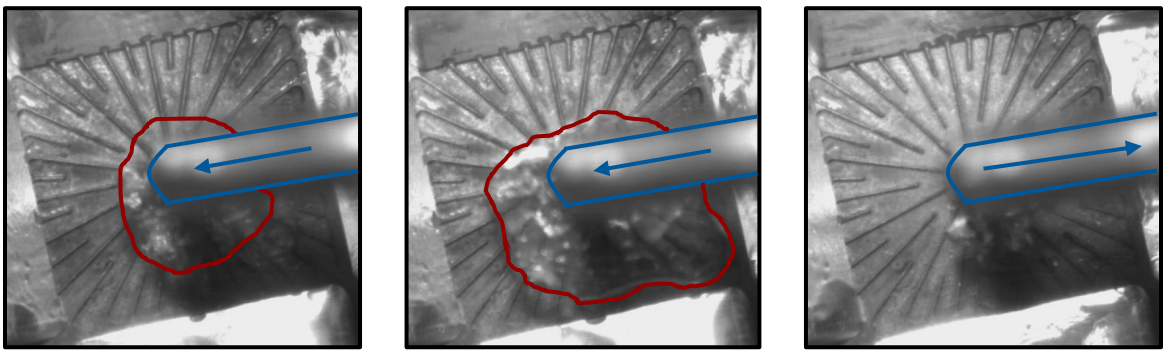

Figure 26. Back flow instability over radial microchannels.

4.4.2 Effect of Gap

The following string of images show the effect of an added gap to the offset strip fin geometry. The goal of the added gap is to increase the area for larger vapor bubbles to rise in order for bubbles to continue to nucleate in the channels. The image seen in Fig. 27 shows the area that will be focused on in the next analyzed images. The first frame of Fig. 27 shows a vapor bubble

expanded over the lower left corner of the geometry. In the next frame, a nucleating bubble can be seen underneath the formed vapor. The next two frames show that bubble detaching from the surface and exiting out the outlet.

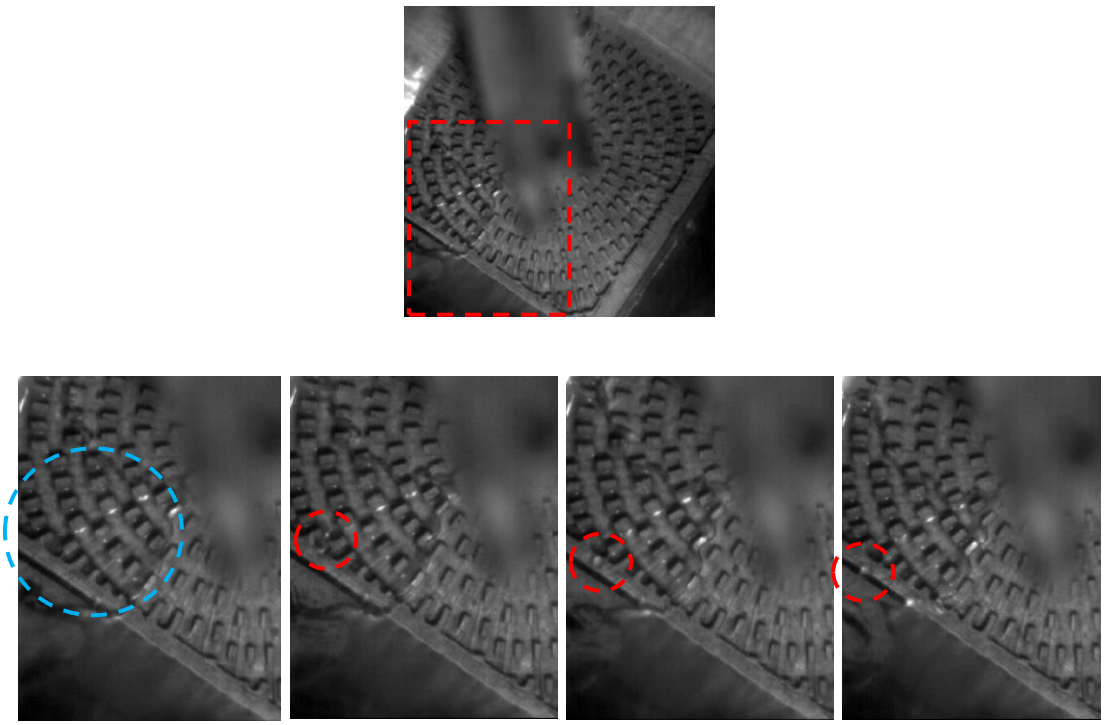

Figure 27. Departing nucleating bubble underneath larger vapor bubble.

4.4.1 Effect of Surface Geometry

The radial offset strip fins have been shown to give better performance than the radial microchannels. The underlying phenomenon attributing to the better performance is two-fold; vapor flow in the circumferential direction and vapor flow in the radial direction.

Due to flow instabilities, pressure difference and design/manufacturing imperfections, in some tests on both surface geometries there is preferential flow. Both cases presented here have a

closed microchannel configuration. If one outlet is experiencing a higher pressure than another, the flow will tend to go towards the path of least resistance. In the radial microchannels, when there is preferential flow towards one outlet, the vapor flows backwards towards the inlet in order to move towards the outlet with a lower pressure difference. The lingering vapor bubble prevents water from touching the surface. This will increase the surface temperature and the pressure drop experienced in the channels. This can be seen in Fig. 28. However, in the offset strip fin geometry, the preferential flow towards one outlet becomes less of a problem due to the increased flow area on the surface. Instead of flowing up one channel and down another, the vapor is free to move throughout the strip fins quickly towards the outlet. This allows the fluid to move more freely throughout the system without fear of dryout or massive vapor coalescence. This can be seen in Fig. 29.

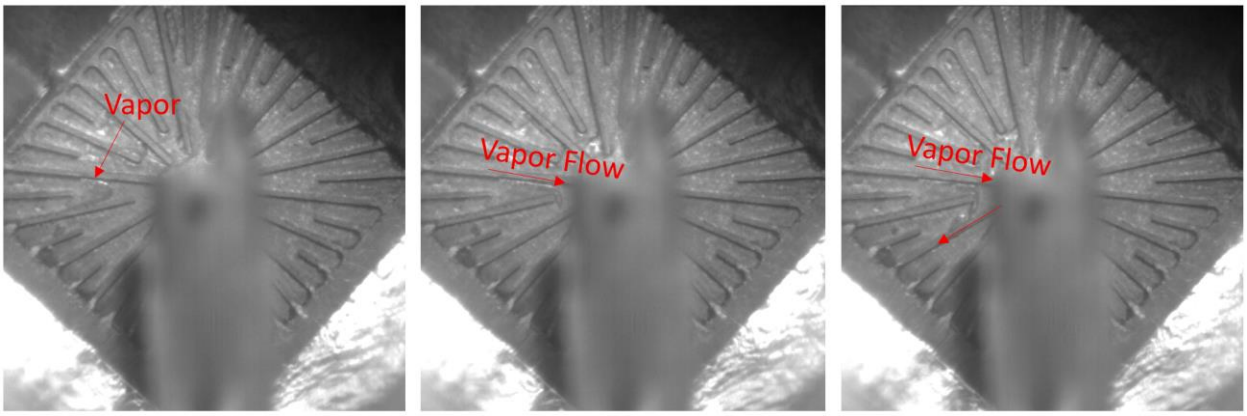

Figure 28. Back flow instabilities and preferential vapor flow through radial microchannels.

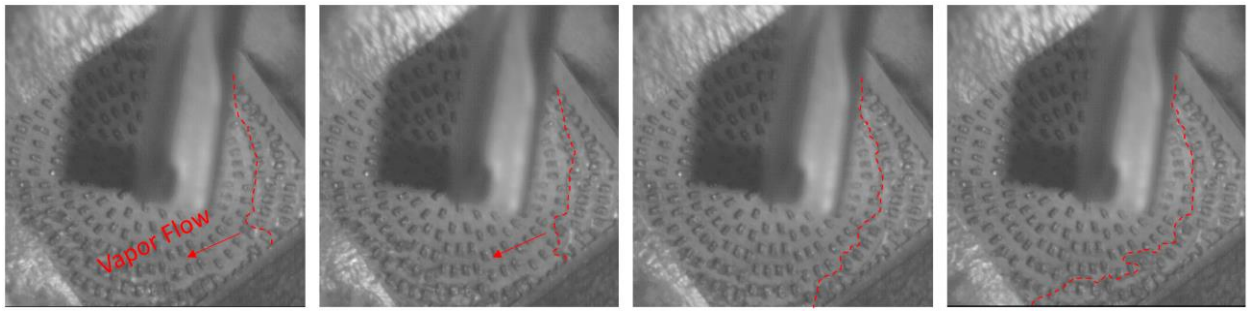

Figure 29. Preferential vapor flow through radial offset strip fins.

The series of images seen in Figure 30 show the vapor flow in the radial direction during nucleate boiling. The first image shows a large vapor bubble covering a majority of chip side. In the following image, the vapor bubble is moving towards the outlet. The third images features the separate bubble streams forming on the downstream side of the offset strip fins. There are four fins where this phenomena can be visualized. And finally the fourth image shows all vapor exiting through the outlet. The higher heat flux achieved by offset strip fins can be attributed to this phenomena. The larger vapor bubbles created by rapid coalescence during the boiling process are broken up and separated by the offset strip fins allowing more fluid to flow throughout the system and preventing dryout or vapor expansion.

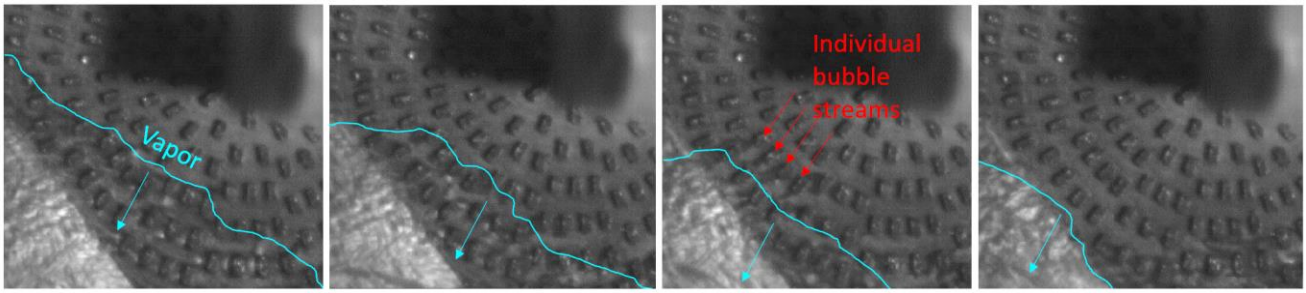

Figure 30. Vapor layer broken up by offset strip fins.

Chapter 5: Conclusion

In this study, two separate geometries were explored in a flow boiling setup; radial microchannels and radial offset strip fins. Initially, a cover plate with a central inlet and two outlets was used but a newer cover plate with four outlets was designed to reduce pressure drop and flow instabilities. Three different configurations were tested with the cover plate touching the copper surface (closed channels), an added gap (open channels) and an added countersink for additional pressure drop. These configurations were experimentally investigated to evaluate their heat transfer and pressure drop performance. The tests covered a wide range of parameters to study their effect on flow rate, gap size and surface geometries. High speed visualization was also undertaken to identify the underlying bubble mechanism for both geometries. The following points were drawn from this study:

1. Radial microchannel geometry was designed, fabricated and tested experimentally at different flow rates. The purpose of the radial geometry was to reduce the overall pressure drop of the system. However, low heat transfer performance was obtained due to flow maldistribution and instability.
    a. The highest heat flux achieved using the radial geometry at a flow rate of 400 mL/min with the older manifold was 267.5 W/cm^2 at ΔT of 49.7°C.
    b. The second manifold and gap configuration improved this performance to 368.8 W/cm^2 at ΔT of 48.7°C. These values were achieved using a flow rate of 240 mL/min.
2. Radial offset strip fins were also fabricated and tested experimentally. The performance obtained was significantly higher than the radial microchannel.

a. Using the first manifold configuration, a maximum heat flux of 306.6 W/cm^2 at ΔT of 24.3°C was achieved. Although the heat flux is not too much higher than the radial microchannel geometry, the massive difference between the two surfaces is the wall superheat. The radial microchannels had a ΔT twice as large as the offset strip fins.

b. A change in manifold with the addition of a gap achieved a heat flux of 897.2 W/cm^2 at ΔT of 63.7°C. Despite the vast increase in heat transfer performance, higher pressure drop values of 190 kPa were recorded.

3. Based on previous study in literature a gap was added over the test surface. The added gap created an open microchannel configuration which allowed for extra area for vapor to escape. This attributed to an even lower pressure drop within the channels and an added countersink at the inlet reduced the pressure drop even further.
4. The addition of a gap reduced the pressure drop and increased the heat transfer performance. The results for the flow rate of 240 mL/min are discussed.

    a. Using manifold two and closed microchannels, offset strip fins yielded a q" of 684 W/cm^2 at ΔT of 40.5°C. The addition of a gap significantly reduced the wall superheat values. A heat flux of 618.3 W/cm^2 at ΔT of 20.1°C was achieved. Although the heat flux decreased slightly with the addition of the gap, the wall superheat for the open geometry is about half the size of the closed geometry.

    b. For the closed geometry, a pressure drop of approximately 175 kPa was seen while the open geometry saw a massive reduction in pressure drop of 13.8 kPa for the same flow rate.

5. An increase in flow rate increased the heat transfer performance as well as the pressure drop. Higher flow rates were used in order to mitigate instabilities seen in the channels. Results for offset strip fins with the second manifold and an open microchannel configuration are presented. At the lower flow rate of 120 mL/min, a q" of 310.4 W/cm^2 at ΔT of 14.7°C is achieved while the higher flow rate of 320 mL/min yields a q" of 897.2 W/cm^2 at ΔT of 63.7°C. A larger flow increases the dissipated heat flux while also increasing the wall superheat. However, an undesirable effect of a higher flow rate is a higher pressure drop. The pressure drop increases from the lowest flow rate of 120 mL/min at 6.9 kPa to the highest of 320 mL/min at 190 kPa.
6. High speed visualization revealed that the offset strip fins yielded better heat transfer performance due to the vapor flow in the radial direction and the vapor flow in the circumferential direction. Not only is there more area for vapor to flow towards the outlet with the lowest pressure drop but the fins separate the coalesced vapor bubble into smaller bubbles. This prevents dryout and allows the fluid to cool the heated surface.
7. A maximum heat flux of ~980 W/cm^2 was achieved at a wall superheat of 51°C using the offset strip fin geometry and the open microchannel configuration with the added inlet countersink. Further modifications to the manifold could yield CHF values beyond 1 kW/cm^2 at pressure drop as low as 20 kPa.

Chapter 6: Future Work

In the current study, radial microchannel and radial offset strip fins were experimentally investigated to enhance heat transfer performance for electronics cooling application. Below presented are some suggestions for future work, based on the understanding obtained from the current research:

6.1 Experimental work: Test setup modifications

The current experimental test setup, seen in Fig. 9, has many positive attributes including ease of manufacturing, high effectiveness and low cost components. However, there are several flaws in the system that could be changed for future studies. Achieving a perfect seal between the manifold and copper test surface can be quite a challenge. Design changes for the manifold or copper block could alleviate some of these strains. One significant problem faced during testing involved the maximum attainable power of the cartridge heaters used. Altering the physical design of the copper block or utilizing higher powered cartridge heaters can assist in the furthering of heat transfer performance. Finally, the thermocouples used for data collection are incredibly effective but also fragile. Due to the arrangement of items in the block, bending a thermocouple (whether accidental or on purpose) is incredible easy. Too much bending can cause the thermocouples to snap and become ineffective. In order to solve this simple problem, different wire thermocouples could be utilized instead of probes or a rearrangement of the test setup should take place.

6.2 Experimental work: Manifold modifications

The addition of the gap resulted in a significant reduction in pressure drop values and an increment in heat transfer performance. The addition of a slight countersink at the inlet improved these characteristics even further. Increasing the gap beyond 127 μm could increase the heat

transfer while reducing the pressure drop. Adding a larger reverse taper expanding from the inlet to all four outlets will create a more uniform area distribution throughout the channels and manifold. A schematic of the reversed taper can be seen in Figure 31.

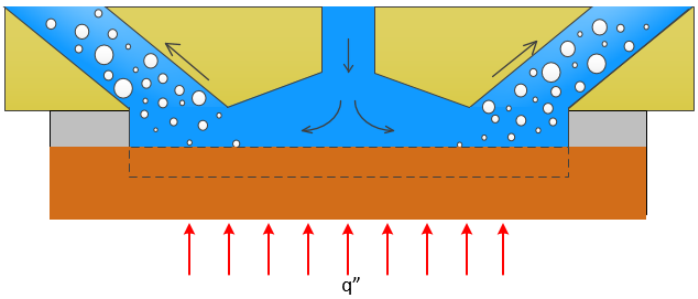

Figure 31. Open microchannel configuration (side view) with added reverse taper, central inlet and outlets (x4).

6.3 Experimental work: Surface geometry

Further design modifications to the surface itself could yield promising results. The radial channels (200 μm in width, 200 μm in depth) were dimensioned based off of previous works while the offset strip fins were dimensioned based on the radial microchannels. An arbitrary length of 350 μm was chosen for the offset strip fins. Now that a better understanding has been obtained for the flow patterns of radial offset strip fins, a further study into the effect of fin dimensions could yield differing results.

6.4 Theoretical model: Pressure drop model

To further explore the effects of pressure drop throughout the system, a theoretical pressure drop analysis can provide insight into the actual reductions created by changing the surface geometry and manifold configurations. Similar to the study performed by Kalani and Kandlikar [53], a homogenous pressure drop model can assist in the exploration of the effects of an added gap and taper in the manifold.

Chapter 7: References

[1] Nukiyama, S., 1934, “Maximum and minimum values of heat q transmitted from metal to boiling water under atmospheric pressure.,” Jpn. Soc. Mech. Eng., **37**(53–54), pp. 367–374.

[2] “Forschung” [Online]. Available: http://129.187.45.233/tum-td/de/forschung/themen/subcooled_flow_boiling. [Accessed: 24-Apr-2016].

[3] Harirchian, T., and Garimella, S. V., 2009, “Effects of channel dimension, heat flux, and mass flux on flow boiling regimes in microchannels,” Int. J. Multiph. Flow, **35**(4), pp. 349–362.

[4] Kandlikar, S. G., and Grande, W. J., 2002, “EVOLUTION OF MICROCHANNEL FLOW PASSAGES-THERMOHYDRAULIC PERFORMANCE,” Technology and Society and Engineering Business Management–2002: Presented at the 2002 ASME International Mechanical Engineering Congress and Exposition, November 17-22, 2002, New Orleans, Louisiana, American Society of Mechanical Engineers, p. 59.

[5] Wang, G. D., Cheng, P., and Wu, H. Y., 2007, “Further Experimental Studies on Flow Boiling Instabilities in Parallel Microchannels,” 2007 First International Conference on Integration and Commercialization of Micro and Nanosystems, American Society of Mechanical Engineers, pp. 965–970.

[6] Deng, D., Wan, W., Tang, Y., Wan, Z., and Liang, D., 2015, “Experimental investigations on flow boiling performance of reentrant and rectangular microchannels – A comparative study,” Int. J. Heat Mass Transf., **82**, pp. 435–446.

[7] Yuan, M., Wei, J., Xue, Y., and Fang, J., “Subcooled Flow Boiling Heat Transfer of FC-72 from Silicon Chips Fabricated with Micro Pin Fins,” Int. J. Therm. Sci., **48**(7), pp. 1416–1422.

[8] Krishnamurthy, S., and Peles, Y., 2010, “Flow Boiling Heat Transfer on Micro Pin Fins Entrenched in a Microchannel,” J. Heat Transf., **132**(4), p. 41007.

[9] Niklas, M., and Favre-Marinet, M., 2005, “An Experimental Study and Numerical Modeling of the Flow in a Network of Triangular Microchannels,” Heat Transf. Eng., **26**(8), pp. 15–23.

[10] Chu, J.-C., Teng, J.-T., and Greif, R., 2010, “Experimental and numerical study on the flow characteristics in curved rectangular microchannels,” Appl. Therm. Eng., **30**(13), pp. 1558–1566.

[11] Sui, Y., Lee, P. S., and Teo, C. J., 2011, “An experimental study of flow friction and heat transfer in wavy microchannels with rectangular cross section,” Int. J. Therm. Sci., **50**(12), pp. 2473–2482.

[12] Chai, L., Xia, G., and Qi, J., 2012, "Experimental and Numerical Study of Flow and Heat Transfer in Trapezoidal Microchannels," Heat Transf. Eng., **33**(11), pp. 972–981.

[13] Steinke, M. E., and Kandlikar, S. G., 2004, "An Experimental Investigation of Flow Boiling Characteristics of Water in Parallel Microchannels," J. Heat Transf., **126**(4), p. 518.

[14] Kandlikar, S. G., "Fundamental Issues Related to Flow Boiling in Minichannels and Microchannels," Exp. Therm. Fluid Sci., **26**(2–4), pp. 389–407.

[15] Kandlikar, S. G., 2006, "Nucleation characteristics and stability considerations during flow boiling in microchannels," Exp. Therm. Fluid Sci., **30**(5), pp. 441–447.

[16] Qu, W., and Mudawar, I., "Measurement and Prediction of Pressure Drop in Two-Phase Microchannel Heat Sinks," Int. J. Heat Mass Transf., **46**(15), pp. 2737–2753.

[17] Hetsroni, G., Mosyak, A., Segal, Z., and Ziskind, G., 2002, "A uniform temperature heat sink for cooling of electronic devices," Int. J. Heat Mass Transf., **45**(16), pp. 3275–3286.

[18] Bergles, A. E., and Kandlikar, S. G., 2003, "Critical heat flux in microchannels: experimental issues and guidelines for measurement," ASME 2003 1st International Conference on Microchannels and Minichannels, American Society of Mechanical Engineers, pp. 141–147.

[19] Kandlikar, S. G., Kuan, W. K., Willistein, D. A., and Borrelli, J., 2006, "Stabilization of Flow Boiling in Microchannels Using Pressure Drop Elements and Fabricated Nucleation Sites," J. Heat Transf., **128**(4), p. 389.

[20] Lu, C. T., and Pan, C., 2011, "Convective boiling in a parallel microchannel heat sink with a diverging cross section and artificial nucleation sites," Exp. Therm. Fluid Sci., **35**(5), pp. 810–815.

[21] Balasubramanian, K., Lee, P. S., Teo, C. J., and Chou, S. K., 2013, "Flow boiling heat transfer and pressure drop in stepped fin microchannels," Int. J. Heat Mass Transf., **67**, pp. 234–252.

[22] Renaud, L., Malhaire, C., Kleimann, P., Barbier, D., and Morin, P., 2008, "Theoretical and experimental studies of microflows in silicon microchannels," Mater. Sci. Eng. C, **28**(5–6), pp. 910–917.

[23] Daniels, B., Liburdy, J. A., and Pence, D. V., 2007, "Adiabatic Flow Boiling in Fractal-Like Microchannels," Heat Transf. Eng., **28**(10), pp. 817–825.

[24] Xiao, B., and Yu, B., 2007, "A fractal analysis of subcooled flow boiling heat transfer," Int. J. Multiph. Flow, **33**(10), pp. 1126–1139.

[25] Favre-Marinet, M., Drobniak, S., Asendrych, D., Gamrat, G., and Niklas, M., 2008, "Numerical and Experimental Investigations of Momentum and Heat Transfer in

Microchannels," ASME 2008 6th International Conference on Nanochannels, Microchannels, and Minichannels, American Society of Mechanical Engineers, pp. 1813–1820.

[26] Krishnamurthy, S., and Peles, Y., 2010, "Flow Boiling Heat Transfer on Micro Pin Fins Entrenched in a Microchannel," J. Heat Transf., **132**(4), p. 41007.

[27] Reeser, A., Bar-Cohen, A., and Hetsroni, G., 2014, "High quality flow boiling heat transfer and pressure drop in microgap pin fin arrays," Int. J. Heat Mass Transf., **78**, pp. 974–985.

[28] Wang, Y., and Peles, Y., 2015, "Subcooled flow boiling in a microchannel with a pin fin and a liquid jet in crossflow," Int. J. Heat Mass Transf., **86**, pp. 165–173.

[29] McNeil, D. A., Raeisi, A. H., Kew, P. A., and Hamed, R. S., 2014, "An investigation into flow boiling heat transfer and pressure drop in a pin–finned heat sink," Int. J. Multiph. Flow, **67**, pp. 65–84.

[30] Reeser, A., Bar-Cohen, A., and Hetsroni, G., 2014, "High quality flow boiling heat transfer and pressure drop in microgap pin fin arrays," Int. J. Heat Mass Transf., **78**, pp. 974–985.

[31] Ames, F. E., Dvorak, L. A., and Morrow, M. J., 2005, "Turbulent Augmentation of Internal Convection Over Pins in Staggered-Pin Fin Arrays," J. Turbomach., **127**(1), p. 183.

[32] Qu, W., 2008, "Thermal and Hydrodynamic Characteristics of Single-Phase Flow and Flow Boiling in a Staggered Micro-Pin-Fin Array," ASME 2008 6th International Conference on Nanochannels, Microchannels, and Minichannels, American Society of Mechanical Engineers, pp. 1861–1870.

[33] Kim, B., and Sohn, B., 2006, "An experimental study of flow boiling in a rectangular channel with offset strip fins," Int. J. Heat Fluid Flow, **27**(3), pp. 514–521.

[34] Pulvirenti, B., Matalone, A., and Barucca, U., 2010, "Boiling heat transfer in narrow channels with offset strip fins: Application to electronic chipsets cooling," Appl. Therm. Eng., **30**(14–15), pp. 2138–2145.

[35] Ranganayakulu, C., and Kabelac, S., 2015, "Boiling of R134a in a Plate-Fin Heat Exchanger Having Offset Fins," J. Heat Transf., **137**(12), p. 121002.

[36] Mandrusiak, G. D., and Carey, V. P., 1989, "Convective boiling in vertical channels with different offset strip fin geometries," J. Heat Transf., **111**(1), pp. 156–165.

[37] Carey, V. P., and Mandrusiak, G. D., 1986, "Annular film-flow boiling of liquids in a partially heated, vertical channel with offset strip fins," Int. J. Heat Mass Transf., **29**(6), pp. 927–939.

[38] London, A. L., and Shah, R. K., 1968, “Offset Rectangular Plate-Fin Surfaces -- Heat Transfer and Flow Friction Characteristics.”

[39] Mullisen, R. S., and Loehrke, R. I., 1986, “A study of the flow mechanisms responsible for heat transfer enhancement in interrupted-plate heat exchangers,” J. Heat Transf., **108**(2), pp. 377–385.

[40] Sridhar, A., Ong, C. L., Paredes, S., Michel, B., Brunschwiler, T., Parida, P., Colgan, E., Chainer, T., Gorle, C., and Goodson, K. E., 2015, “Thermal Design of a Hierarchical Radially Expanding Cavity for Two-Phase Cooling of Integrated Circuits,” ASME 2015 International Technical Conference and Exhibition on Packaging and Integration of Electronic and Photonic Microsystems collocated with the ASME 2015 13th International Conference on Nanochannels, Microchannels, and Minichannels, American Society of Mechanical Engineers, p. V001T09A039–V001T09A039.

[41] Razelos, P., Das, S., and Krikkis, R. N., 2008, “Enhanced boiling heat transfer using radial fins,” Heat Mass Transf., **44**(6), pp. 705–715.

[42] Bo-Qi, X., 2013, “Prediction of heat transfer of nanofluid on critical heat flux based on fractal geometry,” Chin. Phys. B, **22**(1), p. 14402.

[43] Salakij, S., Liburdy, J. A., Pence, D. V., and Apreotesi, M., 2013, “Modeling in situ vapor extraction during convective boiling in fractal-like branching microchannel networks,” Int. J. Heat Mass Transf., **60**, pp. 700–712.

[44] Alharbi, A. Y., Pence, D. V., and Cullion, R. N., 2004, “Thermal Characteristics of Microscale Fractal-Like Branching Channels,” J. Heat Transf., **126**(5), p. 744.

[45] Pence, D., and Enfield, K., eds., 2004, Inherent Benefits in Microscale Fractal-Like Devices for Enhanced Transport Phenomena, WIT, Southampton ; Boston.

[46] Apreotesi, M., Pence, D., and Liburdy, J., 2007, “Vapor extraction from flow boiling in a fractal-like branching heat sink,” ASME 2007 InterPACK Conference collocated with the ASME/JSME 2007 Thermal Engineering Heat Transfer Summer Conference, American Society of Mechanical Engineers, pp. 321–328.

[47] Liburdy, J. A., Pence, D. V., and Narayanan, V., 2008, “Flow Boiling Characteristics in a Fractal-Like Branching Microchannel Network,” ASME 2008 International Mechanical Engineering Congress and Exposition, American Society of Mechanical Engineers, pp. 97–106.

[48] Ruiz, M., Kunkle, C. M., Padilla, J., and Carey, V. P., 2015, “Boiling Heat Transfer Performance in a Spiraling Radial Inflow Microchannel Cold Plate,” ASME 2015 13th International Conference on Nanochannels, Microchannels, and Minichannels collocated with the ASME 2015 International Technical Conference and Exhibition on Packaging and

Integration of Electronic and Photonic Microsystems, American Society of Mechanical Engineers, p. V001T04A023–V001T04A023.

[49] Schultz, M., Yang, F., Colgan, E., Polastre, R., Dang, B., Tsang, C., Gaynes, M., Parida, P., Knickerbocker, J., and Chainer, T., 2015, "Embedded Two-Phase Cooling of Large 3D Compatible Chips with Radial Channels," ASME 2015 International Technical Conference and Exhibition on Packaging and Integration of Electronic and Photonic Microsystems collocated with the ASME 2015 13th International Conference on Nanochannels, Microchannels, and Minichannels, American Society of Mechanical Engineers, p. V003T10A007–V003T10A007.

[50] Kalani, A., and Kandlikar, S. G., 2013, "Experimental Investigation of Flow Boiling Performance of Open Microchannels with Uniform and Tapered Manifolds (OMM)," ASME Summer Heat Transf. Conf.

[51] Kalani, A., and Kandlikar, S. G., 2015, "Flow patterns and heat transfer mechanisms during flow boiling over open microchannels in tapered manifold (OMM)," Int. J. Heat Mass Transf., **89**, pp. 494–504.

[52] Kalani, A., and Kandlikar, S. G., 2013, "Enhanced pool boiling with ethanol at subatmospheric pressures for electronics cooling," J. Heat Transf., **135**(11), p. 111002.

[53] Kalani, A., and Kandlikar, S. G., 2013, "Preliminary Results of Pressure Drop Modeling During Flow Boiling in Open Microchannels with Uniform and Tapered Manifolds (OMM)," ASME 2013 International Mechanical Engineering Congress and Exposition, American Society of Mechanical Engineers, p. V08CT09A057–V08CT09A057.